NeuroImage: Clinical 7 (2015) 105–113

Contents lists available at ScienceDirect

NeuroImage: Clinical

journal homepage: www.elsevier.com/locate/ynicl

Basal forebrain atrophy correlates with amyloid β burden in Alzheimer's disease

Georg M Kerbler[a], Jürgen Fripp[b], Christopher C Rowe[c], Victor L Villemagne[c,d], Olivier Salvado[b], Stephen Rose[b], Elizabeth J Coulson[a,*], Alzheimer's Disease Neuroimaging Initiative

[a]Queensland Brain Institute, Clem Jones Centre for Ageing Dementia Research, The University of Queensland, Brisbane, Qld 4072, Australia
[b]Commonwealth Scientific and Industrial Research Organisation, Computational Informatics, Brisbane, Qld 4029, Australia
[c]Department of Nuclear Medicine and Centre for PET, Austin Health, Melbourne, Vic. 3084, Australia
[d]Florey Institute of Neuroscience and Mental Health, The University of Melbourne, Melbourne, Vic. 3084, Australia

ARTICLE INFO

Article history:
Received 10 February 2014
Received in revised form 11 June 2014
Accepted 18 November 2014
Available online 27 November 2014

Keywords:
Basal forebrain
Amyloid
Alzheimer's disease
Magnetic resonance imaging
PET

ABSTRACT

The brains of patients suffering from Alzheimer's disease (AD) have three classical pathological hallmarks: amyloid-beta (Aβ) plaques, tau tangles, and neurodegeneration, including that of cholinergic neurons of the basal forebrain. However the relationship between Aβ burden and basal forebrain degeneration has not been extensively studied. To investigate this association, basal forebrain volumes were determined from magnetic resonance images of controls, subjects with amnestic mild cognitive impairment (aMCI) and AD patients enrolled in the longitudinal Alzheimer's Disease Neuroimaging Initiative (ADNI) and Australian Imaging, Biomarkers and Lifestyle (AIBL) studies. In the AIBL cohort, these volumes were correlated within groups to neocortical gray matter retention of Pittsburgh compound B (PiB) from positron emission tomography images as a measure of Aβ load. The basal forebrain volumes of AD and aMCI subjects were significantly reduced compared to those of control subjects. Anterior basal forebrain volume was significantly correlated to neocortical PiB retention in AD subjects and aMCI subjects with high Aβ burden, whereas posterior basal forebrain volume was significantly correlated to neocortical PiB retention in control subjects with high Aβ burden. Therefore this study provides new evidence for a correlation between neocortical Aβ accumulation and basal forebrain degeneration. In addition, cluster analysis showed that subjects with a whole basal forebrain volume below a determined cut-off value had a 7 times higher risk of having a worse diagnosis within ~18 months.

1. Introduction

Alzheimer's disease (AD) is a progressive neurodegenerative disorder that results in widespread brain atrophy of both gray and white matter brain regions. Other hallmarks of the disease include the extracellular deposition of amyloid-β (Aβ) and intracellular accumulation of hyper-phosphorylated tau. An emerging method of early diagnosis of AD is to assess brain Aβ burden through Pittsburgh compound B (PiB)–positron emission tomography (PET) imaging. This measure has shown promise in identifying people at risk of developing AD (Villemagne et al., 2011); however, reports of correlations between PiB retention and hippocampal atrophy, the magnetic resonance imaging (MRI) measure most widely used together with traditional cognitive assessment for the diagnosis of AD (Frisoni et al., 2010), have been inconsistent. Therefore it remains unclear what additional factors control the progression to dementia of healthy subjects with high Aβ load.

Cholinergic neurons in the basal forebrain, a gray matter region located in the medial and ventral aspects of the brain, provide the neurotransmitter acetylcholine to a variety of different brain regions. Anterior basal forebrain nuclei, including the medial septum and diagonal band send projections to the hippocampus, olfactory bulb, and piriform and entorhinal cortices. Posterior basal forebrain nuclei, including the nucleus basalis of Meynert project to the amygdala and frontal, cingulate and parietal cortices, as well as to the orbital and occipital cortices and the temporal lobe (Mesulam et al., 1983; Zaborszky et al., 2008). Regulation of acetylcholine supply to these brain regions is involved in local activation and modulation of plasticity, and cholinergic basal forebrain neurons can therefore influence critical behaviors such as attention,

Abbreviations: 3D, 3-dimensional; Aβ, amyloid-beta; AD, Alzheimer's disease; ADNI, Alzheimer's Disease Neuroimaging Initiative; AIBL, Australian Imaging, Biomarkers and Lifestyle Flagship Study of Aging; aMCI, amnestic mild cognitive impairment; CSF, cerebrospinal fluid; GM, gray matter; HC, healthy control; MCI, mild cognitive impairment; MNI, Montreal Neurological Institute; MPM, maximum probability maps; MPRAGE, magnetization prepared rapid gradient echo; MRI, magnetic resonance imaging; OR, odds ratio; PET, positron emission tomography; PiB, Pittsburgh compound B; SPSS, statistics software package for the social sciences; SUVR, standard uptake value ratio; SyN, symmetric normalization; T1W, T1-weighted; TG-ROC, two-graph receiver operating characteristic; WM, white matter.

* Corresponding author at: Queensland Brain Institute, The University of Queensland, Brisbane, Qld 4072, Australia. Tel.: +61 71 33466392; fax: +61 7 33466301.
E-mail address: e.coulson@uq.edu.au (E.J. Coulson).

http://dx.doi.org/10.1016/j.nicl.2014.11.015

learning and memory (Mufson, 2003; Schliebs and Arendt, 2011). Post-mortem assessment has revealed that significant degeneration of these neurons as an early pathological feature of AD patients, and their degeneration, which is likely to underpin aspects of cognitive decline associated with the disease (Contestabile, 2011; Mesulam, 2004; Schliebs and Arendt, 2011), drove the development of the now widely prescribed acetyl cholinesterase inhibitor class of drugs. Consistent with this, recent studies have demonstrated that AD patients, as well as patients with mild cognitive impairment (MCI), a prodromal stage to AD, show significant basal forebrain volume loss compared to age-matched controls (Grothe et al., 2012b; Hall et al., 2008; Muth et al., 2010), with atrophy of discrete regions within the basal forebrain being significantly associated with global cognitive decline as well as delayed recall scores in AD subjects (Grothe et al., 2010). Although the basal forebrain has been shown to degenerate in normal aging, the rate of atrophy is significantly higher in subjects suffering from dementia (Grothe et al., 2012a), and specific areas within the basal forebrain appear to be particularly vulnerable to AD-associated degeneration (Grothe et al., 2012b).

An association between basal forebrain atrophy and Aβ burden in AD has recently been reported using MRI and AV45-PET data (Grothe et al., 2014; Teipel et al., 2014) acquired from the Alzheimer's Disease Neuroimaging Initiative (ADNI) cohort. In this study we also found a significant association between basal forebrain atrophy, based on a histological mask restricted to AD-specific degeneration, and Aβ load using PiB–PET, including a correlation between these hallmarks that extends to healthy control subjects of the Australian Imaging, Biomarkers and Lifestyle (AIBL) cohort (Ellis et al., 2009). Furthermore, we determined that degeneration of the basal forebrain is a significant risk factor for further cognitive decline in control and MCI cohorts, irrespective of Aβ burden.

2. Materials and methods

2.1. Subjects

Data analyzed for this report were obtained from the AIBL study (Ellis et al., 2009) (http://www.aibl.csiro.au/) and the ADNI study (http://adni.loni.ucla.edu). From the AIBL study, longitudinal PiB and 3T T1-weighted (T1W) MRI images of AD, amnestic MCI (aMCI) and healthy control (HC) subjects at two time-points (Table 1) were used. The HC and aMCI groups were further subdivided into subjects with high (PiB+) and low (PiB−) PiB retention levels, as previously reported (Villain et al., 2012). The methodology for cohort recruitment and evaluation has been reported elsewhere (Ellis et al., 2009). From the ADNI-2/GO study, 3 T T1W MRI images of HC, aMCI and AD subjects (Table 2) were examined.

2.2. Imaging protocol

From the ADNI cohort, 3 T MR images were acquired using the magnetization prepared rapid gradient echo (MPRAGE) imaging protocol in accordance with ADNI's guidelines for these scans (http://adni.loni.usc.edu/methods/documents/mri-protocols). For the AIBL cohort, 3 T MR structural images were acquired on a Siemens 3 T Trio. Participants received an MRI scan using the ADNI 3D MPRAGE sequence, with 1×1 mm in-plane resolution and 1.2 mm slice thickness, TR/TE/T1 = 2300/2.98/900, flip angle 9° and field of view 240×256 and 160 slices. In addition, each AIBL subject received ~370 MBq PiB intravenously over 1 min. A 30-minute acquisition in 3-dimensional (3D) mode starting 40 min after injection of PiB was performed with a Philips Allegro PET camera. A transmission scan was performed for attenuation correction. PET images were reconstructed using a 3D RAMLA algorithm.

Table 2
Demographics of the ADNI cohort. There was a significant difference for age between the AD and aMCI groups. Subject groups did not differ based on gender or years of education. For representation of the healthy population we set CDR = 0 as the criterion for the HC groups at baseline. Age and MMSE scores are expressed as mean ± SD.

ADNI study			
	HC	aMCI	AD
Number of subjects	69	127	30
Age	73.5 ± 6.7	72.3 ± 8.2	77.1 ± 7.5
Sex F/M	41/28	53/74	13/17
MMSE	28.9 ± 1.2	28.3 ± 1.5	23.4 ± 2.1
CDR	0	0–1	0.5–1

2.3. MRI processing

The hippocampus, pons and gray matter (GM), white matter (WM) and cerebrospinal fluid (CSF) were segmented from the MPRAGE images using the method outlined in Bourgeat et al. (2010). A skull strip mask was generated from the GM, WM and CSF segmentation. All volume calculations reported are normalized by intracranial volume.

Using the AIBL study data, the skull-stripped MPRAGE images of all subjects were normalized to create an average elderly template brain using the open-source deformable registration tool ANTS. ANTS provides functionality for generating optimal templates, given a collection of images, which offers advantages over a priori templates for image normalization (for instance in the hippocampus; Avants et al., 2010). The population-specific template was generated by iteratively registering images to the current template estimate. A new shape and intensity average were then computed from the results of the registrations and the current template estimate was set as the average. This template generation procedure was repeated iteratively (I = 5). Each registration in this procedure used the greedy symmetric normalization algorithm (SyN, parameters outlined below) and the cross-correlation after subtracting the local mean from the image match metric. A *z*-score map of the deformation field of the AD subjects with HC subjects from the AIBL cohort was generated.

The registration between each subject's MPRAGE image (AIBL and ADNI) and the population-specific template was performed using the SyN algorithm (GradStep = 0.5, regularization sigma = 2.0). The

Table 1
Demographics of AIBL cohort at baseline and follow up. Numbers in brackets at baseline indicate the number of subjects used for calculation of longitudinal changes. At baseline, the ages of the HC PiB− and HC PiB+ subjects($p < 0.05$), as well as the HC PiB− and aMCI($p < 0.001$) subjects, were significantly different. There was no gender difference between groups. Mini-mental state examination (MMSE) scores between aMCI/AD and all other groups were significantly different. Years of education were not significantly different between groups. For representation of the healthy population we set clinical dementia rating (CDR) = 0 as the criterion for the HC groups at baseline. Age and MMSE scores are expressed as mean ± SD.

AIBL study								
	Baseline				Follow up (~18 months)			
	HC PiB-	HC PiB+	aMCI	AD	HC PiB−	HC PiB+	aMCI	AD
Number of subjects	101 (89)	44 (35)	40 (21)	38 (16)	83	39	17	22
Age	71.1 ± 6.7	75.1 ± 6.8	76.5 ± 7.2	72.5 ± 8.5	72.2 ± 6.5	74.9 ± 7.0	77.0 ± 6.8	74.3 ± 7.9
Sex F/M	57/44	23/21	20/20	22/16	49/34	14/25	9/8	11/11
MMSE	28.8 ± 1.2	28.8 ± 1.2	27.3 ± 2.2	20.6 ± 5.2	28.8 ± 1.4	28.5 ± 1.5	27.4 ± 2.0	20 ± 5.7
CDR	0	0	0.5	0.5–3	0	0–0.5	0–0.5	0.5–2

image match metric was the cross-correlation between the images. Cross-correlation after subtracting the local mean from the image at each voxel was computed using a $5 \times 5 \times 5$ voxel window. Registration was performed in a multi-resolution scheme, with a maximum of 30 iterations at 4× subsampling, 90 iterations at 2× subsampling, and 50 iterations at full resolution.

To establish basal forebrain masks encompassing only those areas that undergo atrophy in AD patients (Fig. 1), we compared all control and AD subjects from the AIBL cohort and overlaid the resultant *z*-score map (set to −0.5 and −1 standard deviations) on a standard Montreal Neurological Institute (MNI) brain (*z*-score map, Fig. 1A, B). Using published probabilistic basal forebrain maps derived from histological data as a guide for the limits of the structure (Zaborszky et al., 2008), we then manually segmented the regions of atrophy within the standard space corresponding to the basal forebrain area. Using this method we created two types of basal forebrain masks.

First, we used published raw probabilistic maps (Zaborszky et al., 2008) from at least one post-mortem brain as a guide, resulting in a basal forebrain mask covering a large number of basal forebrain voxels (BF raw; size: 3193 voxels; Fig. 1A, B) and a final delineated area of intermediate anatomical specificity. Second, we used maximum probability maps (MPMs; Zaborszky et al., 2008) as guidance, resulting in a basal forebrain mask covering voxels that were identified as lying in the basal forebrain in ten post-mortem brains (BF MPM; size: 1160 voxels; Fig. 1A, B) and a final delineated area of high anatomical specificity. One aim of this study was to assess and compare the sensitivity of

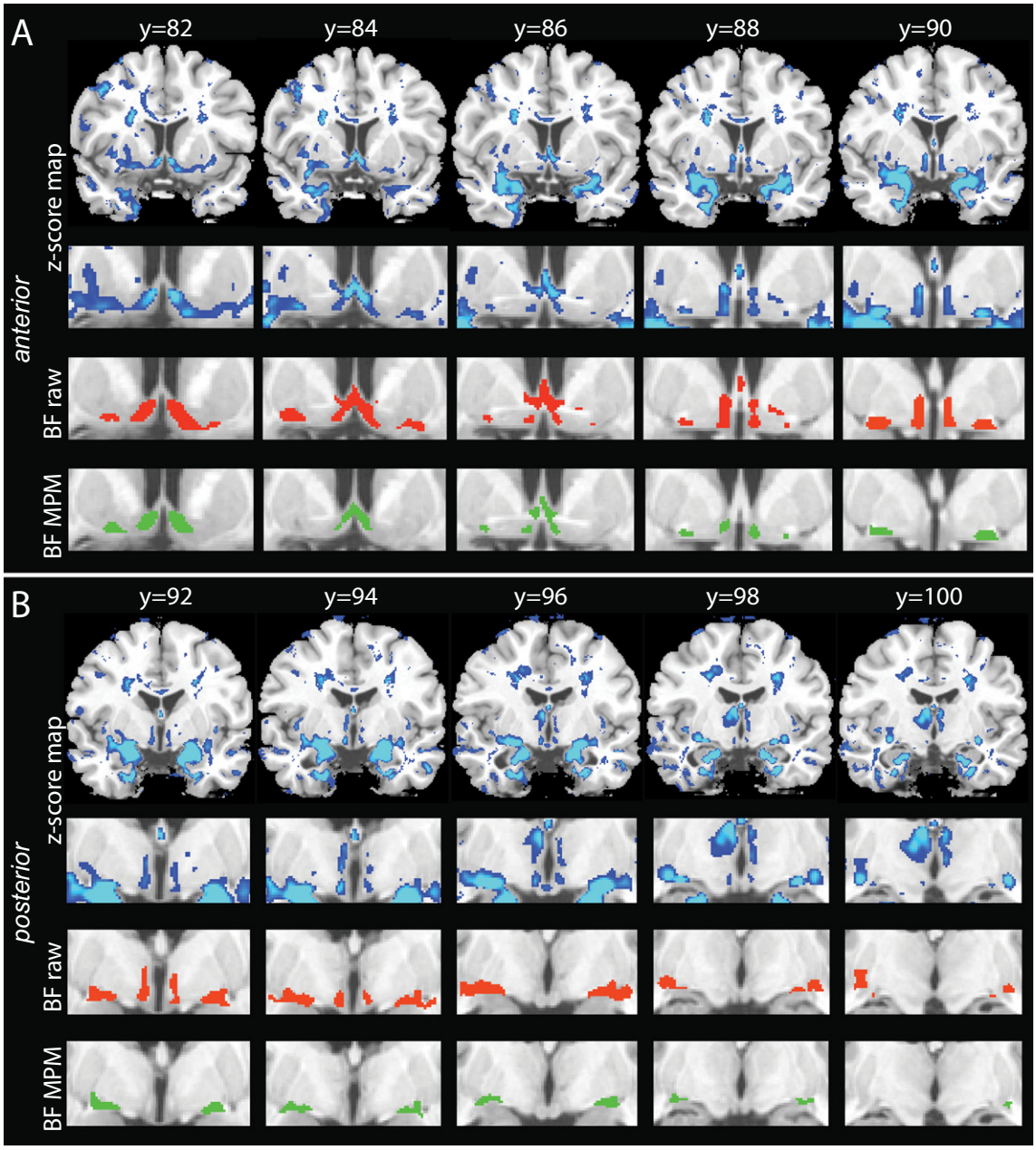

Fig. 1. Basal forebrain masks of AD-specific changes in template space. Coronal slices illustrating the *z*-score map on a whole template brain (blue; top row A and B) calculated by comparing the HC and AD groups in the AIBL study. In the lower rows (A, B), a magnified view of the basal forebrain area is shown to better illustrate the *z*-score map (blue) as well as individual basal forebrain volumes. The BF raw mask (red; A, B) was used as a combination of the anterior and posterior parts for analysis of the whole basal forebrain area. The BF MPM mask (green; A, B) was used both as a combination of the anterior and posterior regions, and the anterior and posterior regions individually, to analyze the basal forebrain area. The same slices at different levels from rostral to caudal are shown in A and B, on a T1-weighted image. BF = basal forebrain, MPM = maximum probability map.

both BF raw and MPM masks in detecting volumetric changes as well as identifying associations with global Aβ burden. To study anterior and posterior basal forebrain compartments separately, we further divided the BF MPM map into an anterior BF MPM volume (size: 595 voxels; Fig. 1A), covering Ch1–3 as well as Ch4 anterior cell groups, and a posterior BF MPM volume (size: 565 voxels; Fig. 1B), covering Ch4 intermediate and posterior cell groups (nomenclature according to Mesulam et al., 1983). The final BF raw and BF MPM masks comprised areas throughout the entire extent of the basal forebrain area (Ch1–4 cell groups) and were validated by overlaying the masks onto newly developed raw probabilistic and MPM basal forebrain post-mortem maps (Eickhoff et al., 2005, 2006, 2007), respectively. This showed an overlap of 50% for the BF raw mask with the raw probabilistic post-mortem map, an overlap of 85% for the BF MPM map with the raw probabilistic post-mortem map and an overlap of 46% for the BF MPM map with the MPM post-mortem map. Neither the BF raw nor the BF MPM map was specific for cholinergic cells of the basal forebrain, but rather represented the general basal forebrain area. Using the aforementioned registration between the subject and atlas, the basal forebrain masks were propagated into the subjects' space and any voxels labeled as CSF (from CSF segmentation) were removed. The resulting mask was then used to extract the GM volume.

Because the basal forebrain masks were created based on atrophy maps derived from comparing AD and control subjects from the AIBL cohort, we tested whether the BF raw mask was able to detect changes in the AIBL cohort as well as in an independent cohort, namely the ADNI cohort (Fig. 2). This analysis revealed similar changes between AD and control subjects as well as AD and aMCI subjects in both cohorts.

2.4. PET image processing

The PET images were processed as described by Bourgeat et al. (2010). In summary, PET and MR images were co-registered. The PiB images were standard uptake value ratio (SUVR) normalized (pons WM) with PiB+ defined as SUVR > 0.71 (Villain et al., 2012) and neocortical PiB retention calculated within the GM segmentation.

2.5. Statistical analysis

The Statistics Software Package for the Social Sciences (SPSS, v20.0) was used to determine significant differences and correlations. Group comparisons were performed using ANOVA followed by the Bonferroni post-hoc test. The parameters compared between groups were corrected for age. Partial correlations controlling for age were used to determine significant associations between parameters. There was no significant difference for sex or years of education between groups. Basal forebrain volume, hippocampal volume and neocortical PiB retention values were significantly correlated to age but not sex or years of education.

Hierarchical cluster analysis was used to determine the basal forebrain volumes that distinguished discrete clusters. Two-step cluster analysis automatically identified three existing clusters in the basal forebrain volume data, and both non-hierarchical (K-means) cluster analysis and two-step cluster analysis provided highly similar cluster groups. The two-graph receiver operating characteristic (TG-ROC) was used to determine cut-off values between clusters (Greiner, 1995). The odds ratio (OR) was calculated to determine the probability of subjects being within the high/medium vs. low-risk basal forebrain volume group at baseline if their diagnosis worsened at follow-up. A chi-square test was used to determine the significance of this ratio.

3. Results

3.1. Differences in basal forebrain volume between HC, aMCI and AD subjects

To measure basal forebrain atrophy in this study, four different masks were used (Fig. 1). These masks were based on raw probabilistic (BF raw) and MPM maps (BF MPM, BF MPM anterior and BF MPM posterior) of post-mortem delineations of the basal forebrain, and further restricted to represent basal forebrain areas found to undergo atrophy in AD subjects versus age-matched controls. The results of group comparisons of BF raw volumes in the AIBL and ADNI cohorts (Fig. 2) and group comparisons of BF MPM volumes in the AIBL cohort (Table 3) are shown. All basal forebrain volumes of the AD group were significantly less than those of HC subjects. In addition AD subjects had significantly smaller basal forebrain volumes than aMCI subjects. The BF raw volumes between the HC and aMCI groups in the ADNI cohort were not significantly different. Furthermore all basal forebrain volumes of aMCI subjects were significantly smaller than those of HC PiB− subjects (control subjects showing low PiB retention values), but only the BF raw volume of aMCI subjects was significantly different from that of HC PiB+ subjects (control subjects showing high PiB retention values). To test whether controls at risk of developing AD, according to PiB retention status, namely HC PiB+ subjects, had smaller basal forebrain volumes than HC PiB− subjects, we compared the two groups. No significant difference in the mean basal forebrain volume between the HC PiB+ and HC PiB− groups was detected.

3.2. Correlation between whole basal forebrain volumes and neocortical amyloid burden

To determine whether the volume of the whole basal forebrain area was correlated to the neocortical amyloid level measured by PiB–PET

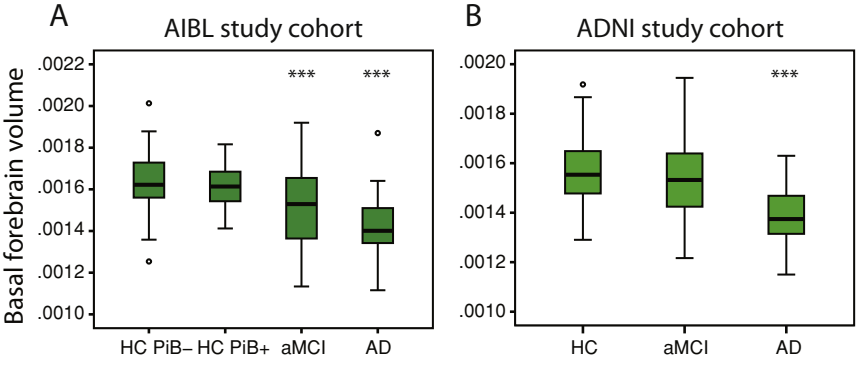

Fig. 2. Group comparisons of basal forebrain volume in the AIBL and ADNI study cohorts. In the AIBL (A) study, the basal forebrain volume was significantly decreased in the AD and aMCI groups compared to controls. In the ADNI study (B), the basal forebrain volume of the AD subject group was significantly smaller than that of the HC and aMCI subject groups. Basal forebrain Volumes of the aMCI groups display high variability in both study cohorts. *** $p < 0.001$. Whiskers represent min/max values except data points (circles) more than 1.5 interquartile ranges away from the 75th percentile.

Table 3
p-Values of group comparisons of basal forebrain volumes in the AIBL cohort. All volumes were significantly different between the AD and control, AD and aMCI as well as aMCI and HC PiB− groups, whereas only the BF raw volume was significantly different between the aMCI and HC PiB+ subjects. BF = basal forebrain, MPM = maximum probability map.

Volume	AD vs HC PiB+	AD vs HC PiB−	AD vs aMCI	aMCI vs HC PiB+	aMCI vs HC PiB−	HC PiB+ vs HC PiB−
BF raw	<0.001	<0.001	0.002	0.02	<0.001	1.0
BF MPM	<0.001	<0.001	0.001	0.151	0.002	1.0
BF MPM anterior	<0.001	<0.001	0.026	0.066	0.001	1.0
BF MPM posterior	<0.001	<0.001	0.021	0.393	0.001	0.385

Table 4
Correlations of basal forebrain volumes to the neocortical PiB retention values in groups of the AIBL cohort. Significant interactions were found for BF raw and BF MPM posterior volumes in the HC PiB+ group, whereas BF raw and BF MPM anterior volumes showed significant interactions in the AD group. Only the BF MPM anterior volume was significantly correlated to neocortical PiB retention in aMCI PiB+ subjects. BF = basal forebrain, MPM = maximum probability map.

Volume		All subjects	HC PiB−	HC PiB+	aMCI	aMCI PiB+	AD
BF raw	r	0.47	0.09	0.32	0.18	0.33	0.39
	p-Value	<0.001	0.36	<0.05	0.27	0.12	<0.05
BF MPM	r	0.46	0.17	0.24	0.26	0.39	0.32
	p-Value	<0.001	0.1	0.12	0.11	0.066	0.053
BF MPM anterior	r	0.43	0.17	0.06	0.23	0.43	0.42
	p-Value	<0.001	0.1	0.71	0.16	<0.05	<0.05
BF MPM posterior	r	0.44	0.13	0.33	0.25	0.29	0.22
	p-Value	<0.001	0.19	<0.05	0.12	0.19	0.19

we performed partial age-controlled correlations between the two measures in the AIBL cohort. Scatter plots of BF raw volume correlations are shown in Fig. 3 and *r*- and *p*-values of BF raw as well as BF MPM volumes are listed in Table 4. We found that, on average, subjects with high Aβ burden, regardless of clinical diagnosis, had smaller BF raw and BF MPM volumes, whereas subjects with low Aβ burden had basal forebrain volumes in the normal range. Correlations in individual groups, namely in the HC (PiB+ and PiB−), aMCI (PiB+ and PiB−) and AD groups revealed that the BF raw volume was correlated to the neocortical PiB retention value in the AD ($r = 0.39$; $p < 0.05$) and HC PiB+ ($r = 0.31$; $p < 0.05$) groups, but not in the aMCI PiB+ ($r = 0.33$; $p = 0.12$), aMCI PiB− ($r = 0.17$; $p = 0.55$) and HC PiB− ($r = 0.09$; $p = 0.36$) groups. In contrast, neither BF MPM volume, nor hippocampal volume (data not shown), was correlated to the neocortical PiB retention in any of the abovementioned groups.

3.3. Correlation between anterior/posterior basal forebrain volumes and neocortical amyloid burden

The anterior basal forebrain volume (BF MPM anterior) represents the medial septum (Ch1 nucleus) and the vertical (Ch2 nucleus) and horizontal diagonal band of Broca (Ch3 nucleus), as well as anterior parts of the nucleus basalis of Meynert (Ch4 nucleus). This volume

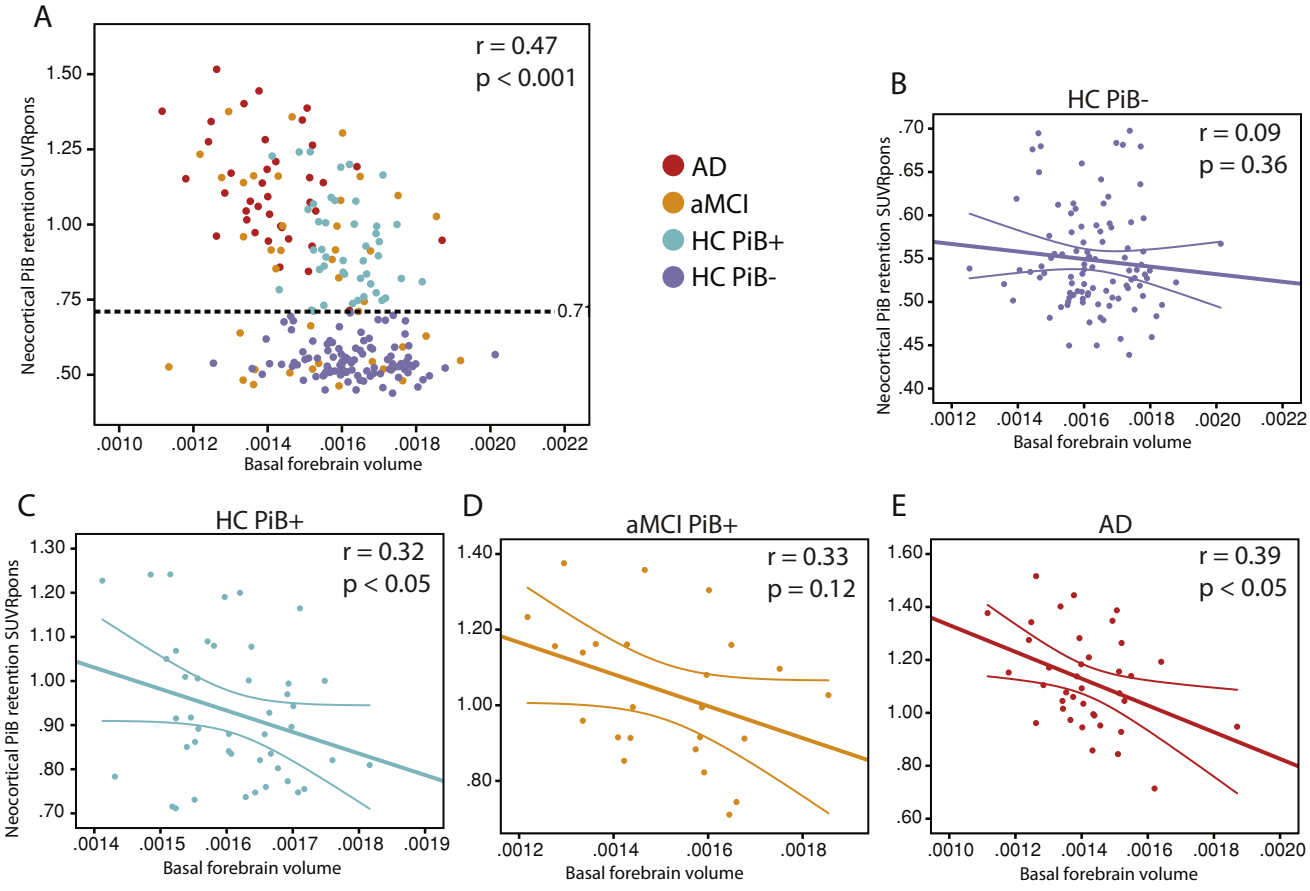

Fig. 3. Correlation of BF raw volume (x-axis) to neocortical PiB retention (y-axis) in the AIBL study. The interaction between the two measures is shown for all subjects pooled together (A) as well for individual subject groups (B–E). The cut-off value used to determine high and low PiB status (0.71) at the baseline time point is indicated in (A) by the horizontal dashed line. Significant interactions were observed in the HC PiB+ (C) and AD (D) subject groups. Even though the correlation coefficient was high in the aMCI PiB+ group, the interaction was not significant. A linear fit line with 95% confidence interval is shown.

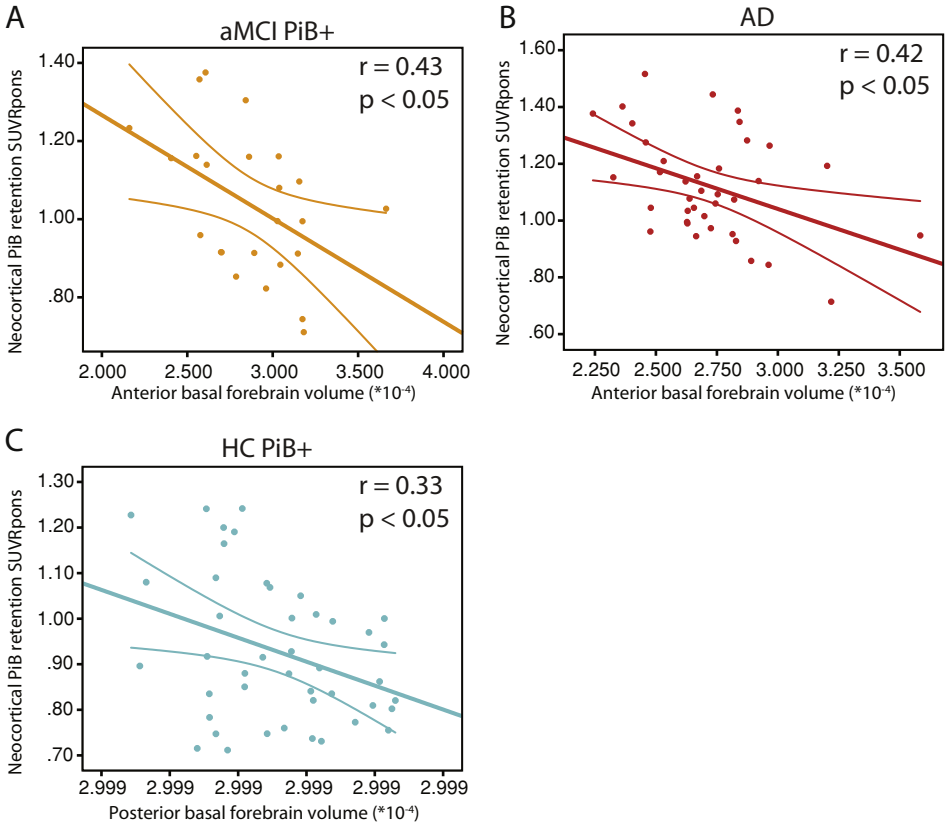

Fig. 4. Significant correlations of anterior and posterior BF MPM posterior Volumes (x-axis) to neocortical PiB retention (y-axis) in the AIBL study. Whereas BF MPM anterior volume showed significant correlations in aMCI PiB+ (A) and AD (B) subjects, BF MPM posterior volume was significantly correlated to neocortical PiB retention in HC PiB+ (C) subjects. A linear fit line with 95% confidence interval is shown.

was significantly correlated to neocortical PiB retention (Fig. 4, Table 4) when pooling all subjects together ($r = 0.43$; $p < 0.001$), as well as in the AD ($r = 0.42$; $p < 0.05$) and aMCI PiB+ ($r = 0.43$; $p < 0.05$) groups but not the HC PiB+ ($r = 0.06$; $p = 0.71$) group alone. Notably the posterior basal forebrain volume (BF MPM posterior), corresponding to intermediate and posterior parts of the NbM (Ch4 nucleus), was correlated to neocortical PiB retention (Fig. 4, Table 4) in all subjects ($r = 0.44$; $p < 0.001$) and HC PiB+ subjects (0.33; $p < 0.05$) alone, but not in the aMCI PiB+ ($r = 0.29$; $p = 0.19$) and AD ($r = 0.22$; $p = 0.19$) subject groups. There was no correlation of either BF MPM anterior or BF MPM posterior volume to neocortical Aβ burden in the HC PiB− and aMCI PiB− groups.

3.4. Basal forebrain cluster analysis for diagnosis of converters

To test the diagnostic potential of basal forebrain volume in identifying subjects at risk of converting from either HC to aMCI, or aMCI to AD clinical status, we performed cluster analysis of basal forebrain volume (BF raw) in the AIBL (Fig. 5) and ADNI (data not shown) cohorts using all subjects, irrespective of diagnostic status. Three clusters of normal, reduced and low basal forebrain volume were revealed, and similar cut-off values were found to separate the clusters in both study cohorts. The mean basal forebrain volume of the AD and the aMCI groups fell into the low and reduced basal forebrain volume clusters, respectively. In addition, the mean basal forebrain volume of the HC subjects who were PiB+ fell within the reduced basal forebrain cluster. Moreover, in both the AIBL and ADNI cohorts, the basal forebrain volumes of subjects whose diagnosis changed from either HC to aMCI (AIBL, $n = 3$), HC to AD (AIBL, $n = 1$) or aMCI to AD (AIBL, $n = 5$; ADNI, $n = 3$) were found in either the low or reduced basal forebrain volume group (with the exception of one PIB+ aMCI subject). Cluster

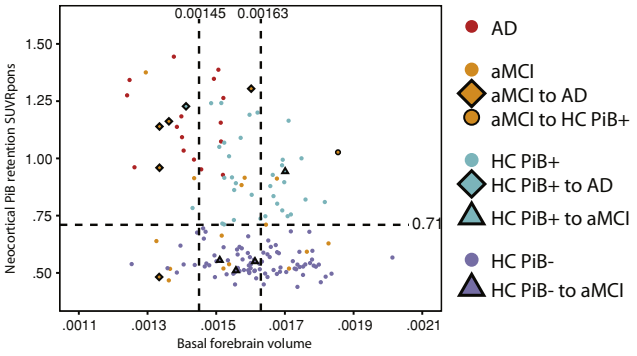

Fig. 5. Delineations based on basal forebrain cluster analysis using the BF raw volume, highlighting the subjects in the AIBL study whose diagnosis worsened ('converters'). In the AIBL study. Basal forebrain cut-off values of 0.00145 and 0.00163 were determined by hierarchical cluster analysis to distinguish three clusters (delineated by vertical dashed lines); the PiB cut-off value of 0.71 is indicated by the horizontal dashed line. Subjects are colored according to their group status at baseline. The mean basal forebrain volume for each group is as follows (given in mean ± SD): AD: 0.001414 ± 0.000138; aMCI: 0.001525 ± 0.000184; HC PiB+: 0.001612 ± 0.000089; HC PiB−: 0.001629 ± 0.000123. The converters are indicated by the diamond-shaped (conversion to AD), triangular (conversion to aMCI) and circular (reversion to HC) data points, with the fill showing the group status at baseline. All but one HC PiB+ to aMCI converting subject fall into the high or medium risk clusters. The subject reverting from aMCI to HC PiB+ group status is shown as a circular data point with a black border. aMCI to AD = aMCI diagnosis at baseline, AD diagnosis at follow up; aMCI to HC PiB+ = aMCI diagnosis at baseline, HC PiB+ diagnosis at follow up; HC PiB+ to AD = HC PiB+ diagnosis at baseline, AD diagnosis at follow up; HC (PiB+ or PiB−) to aMCI = HC diagnosis at baseline, aMCI diagnosis at follow up.

analysis of hippocampal volume (data not shown) revealed that all but 1 PiB− subject, whose diagnosis worsened, fell in either the low or reduced hippocampal volume cluster. Finally, we found that the risk of having a worse diagnosis within ~18 months (based on calculations using AIBL data) was significantly greater (OR = 7.2; chi-squared = 4.53, $p < 0.05$) for subjects falling into either the low or reduced basal forebrain volume category, as compared to subjects with a basal forebrain volume in the normal range.

3.5. Neocortical and cerebellar volume group comparisons and correlations with basal forebrain volume

The AD group was found to have a significantly reduced mean neocortical volume as compared to the HC PiB+ group (Table 5). There were no other neocortical volume differences between groups, and cerebellar volumes were not significantly reduced in any of the subject groups (Table 5). To assess whether basal forebrain atrophy was associated with neocortical atrophy or cerebellar volume, correlations of basal forebrain volumes with neocortical and cerebellar volumes were performed. No significant correlation of basal forebrain volume to either neocortical or cerebellar volume was found.

4. Discussion

Despite AD being characterized by both accumulation of Aβ and atrophy of the basal forebrain, the relationship between these two pathological features has not been widely investigated within independent patient cohorts. We confirm the findings recently published using data from the ADNI cohort (Grothe et al., 2014; Teipel et al., 2014) and demonstrate here that whole basal forebrain volume significantly correlates with neocortical Aβ burden, measured through PiB retention, in AD and HC PiB+ groups. In the HC PiB+ group, neocortical Aβ burden correlates with posterior basal forebrain volume, whereas in aMCI PiB+ and AD groups, neocortical Aβ burden correlates with anterior basal forebrain volume. Furthermore, subjects who retrospectively converted from a diagnosis of either HC to aMCI or aMCI to AD were found to have reduced basal forebrain volumes prior to conversion. These findings provide validity to emerging human and animal studies demonstrating a link between cholinergic basal forebrain neuron degeneration and Aβ production and/or deposition (Gil-Bea et al., 2012; Grothe et al., 2014; Ramos-Rodriguez et al., 2013; Teipel et al., 2014).

The interaction between basal forebrain volume and neocortical Aβ burden was studied using whole, anterior or posterior basal forebrain masks created by delimiting those areas found to undergo atrophy in AD subjects (versus age-matched controls) within the basal forebrain area. However the final masks showed only partial overlap with not yet publicly available post-mortem maps, developed by Eickhoff (Heinrich-Heine University, Düsseldorf) and colleagues, being significantly larger; We acknowledge that this may represent areas of atrophy in anatomically close brain regions in some subjects, but nonetheless, we reasoned that this method of estimating basal forebrain volume may provide increased sensitivity to detect change in AD over the purely post-mortem-based segmentations previously used by others. Indeed, the results of our volumetric analysis using the atrophy-based whole basal forebrain mask are consistent with the findings of previous studies in which subnuclei of the basal forebrain or closely located brain regions were analyzed (Grothe et al., 2010, 2012a,b), with differences in average basal forebrain volume being detected when comparing healthy controls to AD, very mild AD, and MCI groups. The analysis of the ADNI cohort shown here (Fig. 2) further supports data presented previously (George et al., 2011). Interestingly, there was a significant difference between aMCI and HC PiB+ groups for BF raw but not BF MPM volumes in the AIBL cohort. This might be explained by the fact that the BF raw volume is almost three times the size of the BF MPM volume and may therefore be more sensitive to overall changes. The absence of a significant correlation between basal forebrain volume and either neocortical volume or cerebellar volume (Table 5) further strengthens the specificity of basal forebrain degeneration assessed by our measurements as a feature of AD pathology.

In order to investigate whether the correlations between whole basal forebrain volume with neocortical PiB retention observed in this study were driven by interactions with sub-areas of the basal forebrain, we performed correlations of the anterior (Ch1, Ch2, Ch3 and Ch4 anterior nuclei) and posterior (Ch4 intermediate and posterior nuclei) basal forebrain volumes with neocortical PiB retention. In the earliest stages of AD the posterior and intermediate parts of the Ch4 cell group, which are represented by the BF MPM posterior volume in this paper, are the regions predominantly affected by pathological changes (Grothe et al., 2012b). The posterior basal forebrain nuclei send projections to the temporal lobe, amygdala, occipital and orbital cortices, as well as to brain regions subject to heavy Aβ deposition, such as the frontal, cingulate and parietal cortices (Klunk et al., 2004). Furthermore, loss of cholinergic innervation to the aforementioned regions was recently found in vivo in MCI patients (Haense et al., 2012). Thus it is significant that we found a correlation between posterior basal forebrain volume and neocortical PiB retention in the HC PiB+ group, a cohort which represents a control subgroup that might be at high risk of developing AD.

We also observed significant correlations of neocortical PiB retention with BF MPM anterior volume in the aMCI PiB+ and AD groups. In this study, even though the BF raw mask was more sensitive than the BF MPM maps in identifying volumetric differences between groups, BF MPM volumes showed higher correlation coefficients and identified additional significant interactions with neocortical PiB retention as compared to the associations with BF raw volume. In addition, raw probabilistic maps have been shown to be at risk of misclassifying voxels, whereas MPM maps should not suffer from this limitation despite showing similar sensitivity (Eickhoff et al., 2006). Therefore we recommend the use of BF MPM maps, particularly subregional

Table 5
Results of neocortical and cerebellar volume analysis in the AIBL cohort. Average volumes, group comparisons and correlation coefficients of each structure to BF raw volumes are shown. There was a significant difference for neocortical volume between the AD and HC PiB+ group (denoted by *), but not between other groups. We did not find differences in the cerebellar volume and no significant correlation of basal forebrain volume to either neocortical or cerebellar volume was found. Volumes are expressed as mean ± SD.

Group	Neocortex				Cerebellum			
	Volume	Group comparisons		Correlation (r)	Volume	Group comparisons		Correlation (r)
		Vs	p-Value			Vs	p-Value	
HC PiB−	0.433 ± 0.021	HC PiB+	0.3	0.14	0.011 ± 0.001	HC PiB+	1.0	0.08
		aMCI	1.0			aMCI	1.0	
		AD	0.53			AD	1.0	
HC PiB+	0.440 ± 0.018	aMCI	1.0	0.08	0.011 ± 0.001	aMCI	1.0	0.02
		AD	0.02 *			AD	1.0	
aMCI	0.437 ± 0.019	AD	0.13	0.14 (0.18)[a]	0.011 ± 0.001	AD	1.0	0.28 (0.1)[a]
AD	0.426 ± 0.022	HC PiB±	0.02 *	0.12	0.010 ± 0.001	HC PiB±	0.14	0.05

[a] Correlation value for the aMCI PiB+ group is shown in bracket.
* Significant difference at $p < 0.05$.

anterior/posterior volumes, for the future study of associations between global Aβ burden and basal forebrain volumes.

The associations between basal forebrain volumes and amyloid burden presented in this work are consistent with previous reports of a correlation between AV45 retention and basal forebrain volume (Grothe et al., 2014), and the finding that, as subjects progress to aMCI and AD clinical status, changes in anterior basal forebrain areas, containing nuclei that project to the hippocampus, olfactory bulb and piriform and entorhinal cortices, become much more pronounced (Grothe et al., 2012b). In line with this are also recent studies demonstrating cholinergic neuronal dysfunction in the cerebral cortex in MCI and AD based on the use of PET to assess the activity of the key cholinergic enzyme acetylcholine esterase. Acetylcholine esterase is primarily membrane-bound and located on presynaptic cholinergic neurons, and its activity is known to reflect the integrity of the ascending cholinergic system (Garibotto et al., 2013). Degeneration of the cortical cholinergic projection system arising from posterior basal forebrain nuclei, represented by the posterior mask in this paper, was found to occur at early stages of dementia (Haense et al., 2012; Herholz et al., 2008). This is consistent with early dysfunction of posterior nucleus basalis of Meynert neurons, and acetylcholine esterase activity in temporal lobe regions has also been correlated to memory impairment in MCI and AD patients (Haense et al., 2012; Marcone et al., 2012).

While the correlations between basal forebrain volume and neocortical PiB retention reported here may merely reflect the progressive nature of basal forebrain atrophy occurring independently of increasing Aβ load, we hypothesize that this is not the case. Firstly, Aβ burden does not correlate with atrophy of other brain areas, including the hippocampus. Previous work using data from the AIBL study has reported a correlation between hippocampal volume and temporal neocortical PiB retention in the HC PiB+ group (Bourgeat et al., 2010) and subjective cognitively impaired subjects (Chetelat et al., 2010). However, no correlations were found for the AD or the MCI groups, and atrophy of the hippocampus did not correlate with hippocampal PiB retention in another AIBL study (Rowe et al., 2010). Furthermore, similar analyses of AIBL subjects, performed in the present study, failed to reveal any correlation between hippocampal volume and neocortical PiB retention in any subject group (data not shown). Moreover, the correlation in the AD group between BF raw volume and PiB retention increased from $r = 0.39$ to $r = 0.42$ when controlling for hippocampal volume. This indicates that the relationship between basal forebrain volume and Aβ deposition is not driven purely by reduced hippocampal volume, even though these volumes are strongly correlated (data not shown).

Furthermore, in agreement with our findings, a recent study suggested that basal forebrain atrophy can predict cortical amyloid burden, and is more closely associated with cortical amyloid burden than hippocampal atrophy (Teipel et al., 2014). Secondly, a causal relationship is supported by emerging studies in animal models of AD in which cholinergic basal forebrain neuron shrinkage, synaptic loss and axonal degeneration partly caused by, or causing, Aβ deposition in the brain, have been reported (Gil-Bea et al., 2012; Knowles et al., 2009; Ramos-Rodriguez et al., 2013; Sotthibundhu et al., 2008). Although our basal forebrain measurements encompass a structure which is heterogeneous in nature, the cholinergic neurons of the basal forebrain are preferentially lost in AD (Mufson, 2003) and their degeneration could, at least partly, account for the observed reduction in basal forebrain volume. It also remains to be determined what other factors might correlate with or drive basal forebrain volume loss and/or Aβ burden. Of particular relevance is the development of tau pathology that occurs in basal forebrain neurons (Braak et al., 2006; Braak and Del Tredici, 2004, 2011). Tau pathology is more strongly associated with cognitive decline (Braak and Braak, 1991) and is likely to have pronounced effects on basal forebrain volumetric measures.

Regardless of the cause of the observed basal forebrain volume loss, in support of the assertion that early basal forebrain atrophy is a key disease hallmark, cluster analysis of raw BF volume, including analysis of subjects whose diagnosis converted to more cognitively impaired, revealed that most subjects converting from HC to aMCI or from aMCI to AD had a low basal forebrain volume prior to conversion. All converters in both the AIBL and ADNI studies (with the exception of one aMCI PiB+ subject) fell into the low or reduced basal forebrain volume clusters prior to conversion, which could be considered to be the high/medium risk categories. In the AIBL study the mean basal forebrain volumes of AD subjects fell into the low volume cluster whereas mean basal forebrain volumes of the aMCI, HC PiB+ and HC PiB+ groups fell into the reduced volume cluster. Subjects in the latter groups were found in all 3 vol clusters indicating that the range of basal forebrain volumes is large even in non-demented elderly subjects, which is a limitation of using only basal forebrain volumetric measures for diagnostic purposes. Nevertheless we found that subjects belonging to the high/medium risk categories in the AIBL study were 7.2 times more likely to convert to more cognitively impaired than subjects in the low risk category. Interestingly, 3 of the normal controls in the medium risk category who were cognitively impaired at follow up were PiB− at the time of baseline diagnosis, again indicating that basal forebrain atrophy might be a preclinical marker of dementia, albeit that these people may not progress to AD. Although the sample size used to assess basal forebrain volumes for risk of conversion was small, and additional longitudinal data are required to verify our findings, the significant cumulative evidence for basal forebrain atrophy being observed in life in AD clinical cohorts provides increasing impetus for including basal forebrain volume in the general "atrophy signature" for the diagnosis of patients at risk of, or with, AD. Furthermore, basal forebrain measures used in conjunction with other disease markers, such as Aβ load (Kim et al., 2012; Villemagne et al., 2011), may further delineate subjects at risk of progressing to AD or those for whom other interventions, including anti-Aβ treatments, may be of most benefit.

Acknowledgements

GMK was funded by an ANZ Trustees PhD scholarship for medical research and a University of Queensland International Scholarship. EJC was supported by a National Health and Medical Research Council of Australia Career Development Fellowship (569601). This project was funded by a Mason Foundation grant and Queensland State Government National and International Research Alliance Project grant. The study was partially supported by the Commonwealth Scientific Industrial Research Organisation Preventative Health Flagship Program through the Australian Imaging, Biomarkers, and Lifestyle flagship study of aging, the Austin Hospital Medical Research Foundation, Neurosciences Victoria, and the University of Melbourne. The funding sources had no input into the design of this study, the analysis of data, or writing of the manuscript.

Data collection and sharing for this project was funded by the Alzheimer's Disease Neuroimaging Initiative (ADNI) (National Institutes of Health grant U01 AG024904). ADNI is funded by the National Institute on Aging, the National Institute of Biomedical Imaging and Bioengineering, and through generous contributions from the following: Alzheimer's Association; Alzheimer's Drug Discovery Foundation; BioClinica, Inc.; Biogen Idec Inc.; Bristol-Myers Squibb Company; Eisai Inc.; Elan Pharmaceuticals, Inc.; Eli Lilly and Company; F. Hoffmann-La Roche Ltd and its affiliated company Genentech, Inc.; GE Healthcare; Innogenetics, N.V.; IXICO Ltd.; Janssen Alzheimer Immunotherapy Research & Development, LLC; Johnson & Johnson Pharmaceutical Research and Development LLC; Medpace, Inc.; Merck & Co., Inc.; Meso Scale Diagnostics, LLC; NeuroRx Research; Novartis Pharmaceuticals Corporation; Pfizer Inc.; Piramal Imaging; Servier; Synarc Inc.; and Takeda Pharmaceutical Company. The Canadian Institutes of Health Research are providing funds to support ADNI clinical sites in Canada. Private sector contributions are facilitated by the Foundation for the National Institutes of Health (http://www.fnih.org). The grantee organization is the Northern California Institute for Research and Education,

and the study is coordinated by the Alzheimer's disease Cooperative Study at the University of California San Diego. ADNI data are disseminated by the Laboratory for Neuro Imaging at the University of California Los Angeles. This research was also supported by NIH grants P30 AG010129 and K01 AG030514.

We would like to thank Pierrick Bourgeat for helpful discussions and Chris Bell for technical assistance.

References

Avants, B.B., Yushkevich, P., Pluta, J., Minkoff, D., Korczykowski, M., Detre, J., Gee, J.C., 2010. The optimal template effect in hippocampus studies of diseased populations. Neuroimage 49 (3), 2457–2466. http://dx.doi.org/10.1016/j.neuroimage.2009.09.06219818860.

Bourgeat, P., Chételat, G., Villemagne, V.L., Fripp, J., Raniga, P., Pike, K., Acosta, O., Szoeke, C., Ourselin, S., Ames, D., Ellis, K.A., Martins, R.N., Masters, C.L., Rowe, C.C., Salvado, O., 2010. Beta-amyloid burden in the temporal neocortex is related to hippocampal atrophy in elderly subjects without dementia. Neurology 74 (2), 121–127. http://dx.doi.org/10.1212/WNL.0b013e3181c918b520065247.

Braak, H., Alafuzoff, I., Arzberger, T., Kretzschmar, H., Del Tredici, K., 2006. Staging of Alzheimer disease-associated neurofibrillary pathology using paraffin sections and immunocytochemistry. Acta Neuropathol. 112 (4), 389–404. http://dx.doi.org/10.1007/s00401-006-0127-z16906426.

Braak, H., Braak, E., 1991. Neuropathological staging of Alzheimer-related changes. Acta Neuropathol. 82 (4), 239–259. http://dx.doi.org/10.1007/BF003088091759558.

Braak, H., Del Tredici, K., 2004. Alzheimer's disease: intraneuronal alterations precede insoluble amyloid-beta formation. Neurobiol. Aging 25 (6), 713–718. http://dx.doi.org/10.1016/j.neurobiolaging.2003.12.01515165692 [Discussion 743–716].

Braak, H., Del Tredici, K., 2011. The pathological process underlying Alzheimer's disease in individuals under thirty. Acta Neuropathol. 121 (2), 171–181. http://dx.doi.org/10.1007/s00401-010-0789-421170538.

Chételat, G., Villemagne, V.L., Bourgeat, P., Pike, K.E., Jones, G., Ames, D., Ellis, K.A., Szoeke, C., Martins, R.N., O'Keefe, G.J., Salvado, O., Masters, C.L., Rowe, C.C., 2010. Relationship between atrophy and beta-amyloid deposition in Alzheimer disease. Ann. Neurol. 67 (3), 317–324. http://dx.doi.org/10.1002/ana.2195520373343.

Contestabile, A., 2011. The history of the cholinergic hypothesis. Behav. Brain Res. 221 (2), 334–340. http://dx.doi.org/10.1016/j.bbr.2009.12.04420060018.

Eickhoff, S.B., Heim, S., Zilles, K., Amunts, K., 2006. Testing anatomically specified hypotheses in functional imaging using cytoarchitectonic maps. Neuroimage 32 (2), 570–582. http://dx.doi.org/10.1016/j.neuroimage.2006.04.20416781166.

Eickhoff, S.B., Paus, T., Caspers, S., Grosbras, M.H., Evans, A.C., Zilles, K., Amunts, K., 2007. Assignment of functional activations to probabilistic cytoarchitectonic areas revisited. Neuroimage 36 (3), 511–521. http://dx.doi.org/10.1016/j.neuroimage.2007.03.06017499520.

Eickhoff, S.B., Stephan, K.E., Mohlberg, H., Grefkes, C., Fink, G.R., Amunts, K., Zilles, K., 2005. A new SPM toolbox for combining probabilistic cytoarchitectonic maps and functional imaging data. Neuroimage 25 (4), 1325–1335. http://dx.doi.org/10.1016/j.neuroimage.2004.12.03415850749.

Ellis, K.A., Bush, A.I., Darby, D., De Fazio, D., Foster, J., Hudson, P., Lautenschlager, N.T., Lenzo, N., Martins, R.N., Maruff, P., Masters, C., Milner, A., Pike, K., Rowe, C., Savage, G., Szoeke, C., Taddei, K., Villemagne, V., Woodward, M., Ames, D., 2009. The Australian imaging, biomarkers and lifestyle (AIBL) study of aging: methodology and baseline characteristics of 1112 individuals recruited for a longitudinal study of Alzheimer's disease. Int. Psychogeriatr. 21 (4), 672–687. http://dx.doi.org/10.1017/S1041610209009405194702O1.

Frisoni, G.B., Fox, N.C., Jack Jr., C.R., Scheltens, P., Thompson, P.M., 2010. The clinical use of structural MRI in Alzheimer disease. Nat. Rev. Neurol. 6 (2), 67–77. http://dx.doi.org/10.1038/nrneurol.2009.21520139996.

Garibotto, V., Tettamanti, M., Marcone, A., Florea, I., Panzacchi, A., Moresco, R., Virta, J.R., Rinne, J., Cappa, S.F., Perani, D., 2013. Cholinergic activity correlates with reserve proxies in Alzheimer's disease. Neurobiol. Aging 34 (11). http://dx.doi.org/10.1016/j.neurobiolaging.2013.05.02023820589.

George, S., Mufson, E.J., Leurgans, S., Shah, R.C., Ferrari, C., deToledo-Morrell, L., 2011. MRI-based volumetric measurement of the substantia innominata in amnestic MCI and mild AD. Neurobiol. Aging 32 (10), 1756–1764. http://dx.doi.org/10.1016/j.neurobiolaging.2009.11.00620005600.

Gil-Bea, F.J., Gerenu, G., Aisa, B., Kirazov, L.P., Schliebs, R., Ramírez, M.J., 2012. Cholinergic denervation exacerbates amyloid pathology and induces hippocampal atrophy in Tg2576 mice. Neurobiol. Disease 48 (3), 439–446. http://dx.doi.org/10.1016/j.nbd.2012.06.02022759926.

Greiner, M., 1995. Two-graph receiver operating characteristic (TG-ROC): a Microsoft-Excel template for the selection of cut-off values in diagnostic tests. J. Immunol. Methods 185 (1), 145–146. http://dx.doi.org/10.1016/0022-1759(95)00078-O7665897.

Grothe, M., Heinsen, H., Teipel, S., 2012a. Longitudinal measures of cholinergic forebrain atrophy in the transition from healthy aging to Alzheimer's disease. Neurobiol. Aging 34 (4), 1210–1220.

Grothe, M., Heinsen, H., Teipel, S.J., 2012b. Atrophy of the cholinergic basal forebrain over the adult age range and in early stages of Alzheimer's disease. Biol. Psychiatry 71 (9), 805–813. http://dx.doi.org/10.1016/j.biopsych.2011.06.01921816388.

Grothe, M., Zaborszky, L., Atienza, M., Gil-Neciga, E., Rodriguez-Romero, R., Teipel, S.J., Amunts, K., Suarez-Gonzalez, A., Cantero, J.L., 2010. Reduction of basal forebrain cholinergic system parallels cognitive impairment in patients at high risk of developing Alzheimer's disease. Cereb. Cortex 20 (7), 1685–1695. http://dx.doi.org/10.1093/cercor/bhp23219889714.

Grothe, M.J., Ewers, M., Krause, B., Heinsen, H., Teipel, S.J., 2014. Basal forebrain atrophy and cortical amyloid deposition in nondemented elderly subjects. Alzheimers Dement. 10, S344–S353. http://dx.doi.org/10.1016/j.jalz.2013.09.01124418052.

Haense, C., Kalbe, E., Herholz, K., Hohmann, C., Neumaier, B., Krais, R., Heiss, W.D., 2012. Cholinergic system function and cognition in mild cognitive impairment. Neurobiol. Aging 33 (5), 867–877. http://dx.doi.org/10.1016/j.neurobiolaging.2010.08.01520961662.

Hall, A.M., Moore, R.Y., Lopez, O.L., Kuller, L., Becker, J.T., 2008. Basal forebrain atrophy is a presymptomatic marker for Alzheimer's disease. Alzheimers Dement. 4 (4), 271–279. http://dx.doi.org/10.1016/j.jalz.2008.04.00518631978.

Herholz, K., Weisenbach, S., Kalbe, E., 2008. Deficits of the cholinergic system in early AD. Neuropsychologia 46 (6), 1642–1647. http://dx.doi.org/10.1016/j.neuropsychologia.2007.11.02418201734.

Kim, M.J., Lee, K.M., Son, Y.D., Jeon, H.A., Kim, Y.B., Cho, Z.H., 2012. Increased basal forebrain metabolism in mild cognitive impairment: an evidence for brain reserve in incipient dementia. J. Alzheimers Dis. 32 (4), 927–938. http://dx.doi.org/10.3233/JAD-2012-12013322903128.

Klunk, W.E., Engler, H., Nordberg, A., Wang, Y., Blomqvist, G., Holt, D.P., Bergström, M., Savitcheva, I., Huang, G.F., Estrada, S., Ausén, B., Debnath, M.L., Barletta, J., Price, J.C., Sandell, J., Lopresti, B.J., Wall, A., Koivisto, P., Antoni, G., Mathis, C.A., Långström, B., 2004. Imaging brain amyloid in Alzheimer's disease with Pittsburgh Compound-B. Ann. Neurol. 55 (3), 306–319. http://dx.doi.org/10.1002/ana.2000914991808.

Knowles, J.K., Rajadas, J., Nguyen, T.V., Yang, T., LeMieux, M.C., Vander Griend, L., Ishikawa, C., Massa, S.M., Wyss-Coray, T., Longo, F.M., 2009. The p75 neurotrophin receptor promotes amyloid-beta(1–42)-induced neuritic dystrophy in vitro and in vivo. J. Neurosci. 29 (34), 10627–10637. http://dx.doi.org/10.1523/JNEUROSCI.0620-09.200919710315.

Marcone, A., Garibotto, V., Moresco, R.M., Florea, I., Panzacchi, A., Carpinelli, A., Virta, J.R., Tettamanti, M., Borroni, B., Padovani, A., Bertoldo, A., Herholz, K., Rinne, J.O., Cappa, S.F., Perani, D., 2012. [^{11}C]-MP4A PET cholinergic measurements in amnestic mild cognitive impairment, probable Alzheimer's disease, and dementia with Lewy bodies: a Bayesian method and voxel-based analysis. J. Alzheimers Dis. 31 (2), 387–399. http://dx.doi.org/10.3233/JAD-2012-11174822596267.

Mesulam, M., 2004. The cholinergic lesion of Alzheimer's disease: pivotal factor or side show? Learn. Mem. 11 (1), 43–49. http://dx.doi.org/10.1101/lm.69204.

Mesulam, M.M., Mufson, E.J., Levey, A.I., Wainer, B.H., 1983. Cholinergic innervation of cortex by the basal forebrain: cytochemistry and cortical connections of the septal area, diagonal band nuclei, nucleus basalis (substantia innominata), and hypothalamus in the rhesus monkey. J. Comp. Neurol. 214 (2), 170–197. http://dx.doi.org/10.1002/cne.9021402066841683.

Mufson, E.J., 2003. Human cholinergic basal forebrain: chemoanatomy and neurologic dysfunction. J. Chem. Neuroanat. 26 (4), 233–242. http://dx.doi.org/10.1016/S0891-0618(03)00068-114729126.

Muth, K., Schönmeyer, R., Matura, S., Haenschel, C., Schröder, J., Pantel, J., 2010. Mild cognitive impairment in the elderly is associated with volume loss of the cholinergic basal forebrain region. Biol. Psychiatry 67 (6), 588–591. http://dx.doi.org/10.1016/j.biopsych.2009.02.02619375072.

Ramos-Rodriguez, J.J., Pacheco-Herrero, M., Thyssen, D., Murillo-Carretero, M.I., Berrocoso, E., Spires-Jones, T.L., Bacskai, B.J., Garcia-Alloza, M., 2013. Rapid beta-amyloid deposition and cognitive impairment after cholinergic denervation in APP/PS1 mice. J. Neuropathol. Exp. Neurol. 72 (4), 272–285. http://dx.doi.org/10.1097/NEN.0b013e318288a8dd23481704.

Rowe, C.C., Ellis, K.A., Rimajova, M., Bourgeat, P., Pike, K.E., Jones, G., Fripp, J., Tochon-Danguy, H., Morandeau, L., O'Keefe, G., Price, R., Raniga, P., Robins, P., Acosta, O., Lenzo, N., Szoeke, C., Salvado, O., Head, R., Martins, R., Masters, C.L., Ames, D., Villemagne, V.L., 2010. Amyloid imaging results from the Australian imaging, biomarkers and lifestyle (AIBL) study of aging. Neurobiol. Aging 31 (8), 1275–1283. http://dx.doi.org/10.1016/j.neurobiolaging.2010.04.00720472326.

Schliebs, R., Arendt, T., 2011. The cholinergic system in aging and neuronal degeneration. Behav. Brain Res. 221 (2), 555–563. http://dx.doi.org/10.1016/j.bbr.2010.11.05821145918.

Sotthibundhu, A., Sykes, A.M., Fox, B., Underwood, C.K., Thangnipon, W., Coulson, E.J., 2008. Beta-amyloid(1–42) induces neuronal death through the p75 neurotrophin receptor. J. Neurosci. 28 (15), 3941–3946. http://dx.doi.org/10.1523/JNEUROSCI.0350-08.200818400893.

Teipel, S., Heinsen, H., Amaro Jr., E., Grinberg, L.T., Krause, B., Grothe, M., 2014. Cholinergic basal forebrain atrophy predicts amyloid burden in Alzheimer's disease. Neurobiol. Aging 35 (3), 482–491. http://dx.doi.org/10.1016/j.neurobiolaging.2013.09.02924176625.

Villain, N., Chételat, G., Grassiot, B., Bourgeat, P., Jones, G., Ellis, K.A., Ames, D., Martins, R.N., Eustache, F., Salvado, O., Masters, C.L., Rowe, C.C., Villemagne, V.L., 2012. Regional dynamics of amyloid-beta deposition in healthy elderly, mild cognitive impairment and Alzheimer's disease: a voxelwise PiB-PET longitudinal study. Brain 135 (7), 2126–2139. http://dx.doi.org/10.1093/brain/aws12522628162.

Villemagne, V.L., Pike, K.E., Chételat, G., Ellis, K.A., Mulligan, R.S., Bourgeat, P., Ackermann, U., Jones, G., Szoeke, C., Salvado, O., Martins, R., O'Keefe, G., Mathis, C.A., Klunk, W.E., Ames, D., Masters, C.L., Rowe, C.C., 2011. Longitudinal assessment of Abeta and cognition in aging and Alzheimer disease. Ann. Neurol. 69 (1), 181–192. http://dx.doi.org/10.1002/ana.2224821280088.

Zaborszky, L., Hoemke, L., Mohlberg, H., Schleicher, A., Amunts, K., Zilles, K., 2008. Stereotaxic probabilistic maps of the magnocellular cell groups in human basal forebrain. Neuroimage 42 (3), 1127–1141. http://dx.doi.org/10.1016/j.neuroimage.2008.05.05518585468.